MJSAT

Malaysian Journal of Science and Advanced Technology

journal homepage: https://mjsat.com.my/



Malaysia National Energy Transition from the Oil Palm Sector

Andrew Yap Kian Chung*[1], and Nur Sulihatimarsyila Abd Wafti[1]

[1]*Engineering & Processing Division, Malaysian Palm Oil Board, Bangi, Malaysia.*

KEYWORDS

Food-fuel conflicts
National Energy Transition
Net zero
Renewable energy
Sustainability

ARTICLE HISTORY

Received 20 September 2025
Received in revised form 5 October 2026
Accepted 19 October 2026
Available online 2 November 2026

ABSTRACT

The Malaysian government launched the National Energy Policy 2022–2040 on 19 September 2022 to enhance macroeconomic resilience and energy security, promote social equity and affordability, and foster environmental sustainability. The transformation of the energy sector is being carried out within the context of a global energy transition aimed at achieving net-zero emissions by 2050. The potential contribution from the oil palm sector in the energy transition was reviewed. Although renewable energy derived from various oil palm by-products presents no food-fuel conflicts, it remains unscalable due to limitations in planting areas. Treatments of palm biomass could improve fuel properties and marketability. The overall fatty acids methyl esters esterification reaction tends to follow a second-order rate with respect to free fatty acids. Anaerobic digestion of palm oil mill effluent produces biogas. Depending on the available feedstock, processes such as Fischer-Tropsch or hydrotreated esters and fatty acids could generate sustainable aviation fuel. The palm oil industrial premises also offer substantial space for clean solar photovoltaic energy on their rooftops. The energy transition from the oil palm sector requires a comprehensive and collaborative approach that involves all stakeholders.

© 2026 The Authors. Published by Algoritma Sdn. Bhd.
This is an open access article under the CC BY-NC 4.0 license (https://creativecommons.org/licenses/by-nc/4.0/).

1. INTRODUCTION

Climate change is an emerging global challenge that underscores the need for sustainable ecosystems. The energy transition to net zero inevitably requires balancing sustainability, energy security, and financial affordability. The Asia-Pacific region consumes more than half of global energy, with 85% sourced from fossil fuels [1]. In 2014, electricity and heat generation accounted for about 30% of global greenhouse gas emissions [2]. Effective transition models are advancing despite the ongoing energy crisis. However, developing countries face challenges in implementing climate-friendly policies, securing financial support, transferring technology, and achieving economic balance while ensuring a responsible energy transition. Malaysia aims to achieve net-zero emissions by 2050.

The energy transition involves a gradual shift from fossil fuel-dominated energy use to cleaner, renewable energy. Malaysian palm bioenergy potential theoretically meets 64% of the primary energy supply [3]. Various oil palm by-products such as biomass, free fatty acids (FFA), and palm oil mill effluent (POME) can generate renewable energy without raising food-fuel conflicts. This paper succinctly discusses several biomass treatments, reviews various palm oleochemical processes, presents a simulation of FFA esterification for palm biodiesel production, and introduces the feasibility of implementing solar energy in the palm industry.

2. OIL PALM WASTE RESIDUES

Oil palm fronds and trunks produced during pruning, harvesting, and replanting in estates are usually left to degrade in the field for fertilisation [4]. Palm oil mills process the harvested fresh fruit bunches (FFB) to produce crude palm oil (CPO) and palm kernel, while generating about 23% empty fruit bunch (EFB), 13% mesocarp fibre, and 7% kernel shell, which are disposed of as biomass. Oil loss during milling should be controlled as low as reasonably achievable (ALARA), ideally at 1.77% FFB [5] as a baseline for quantifying milling inefficiency. Sludge oil recovery involves

*Corresponding author:
E-mail address: Andrew Yap Kian Chung < andrew@mpob.gov.my >.
https://doi.org/10.56532/mjsat.v6i4.612
2785-8901/ © 2026 The Authors. Published by Algoritma Sdn. Bhd.
This is an open access article under the CC BY-NC 4.0 license (https://creativecommons.org/licenses/by-nc/4.0/).

various operational units, mainly the sludge separator. However, the recoverable amount of non-edible sludge oil is about 1% of FFB. *Table 1* shows the sludge oil specifications [6].

Table 1. PORAM Sludge Oil Specifications

Parameter	Specification Limit
Total Fatty Matter	95% minimum
Moisture and Impurity (M&I)	3.0% maximum
Free Fatty Acids (as Palmitic)	50% minimum

Palm oil mill effluent (POME) is wastewater generated during CPO extraction from FFB. About 600 kg of POME is generated for every 1000 kg of FFB processed [7]. POME is a complex mixture of organic and inorganic compounds whose physical properties vary with several factors, such as the age of the palm fruit bunches, the extraction process used, and the environmental conditions. *Table 2* shows the general POME characteristics [8].

Table 2. Typical Palm Oil Mill Effluent Characteristics

Parameter	[mg L^{-1}]	Mineral	[mg L^{-1}]
Oil and grease (O&G)	4000	Phosphorus (P)	180.00
Biological oxygen demand	25,000	Potassium (K)	2,270.00
Chemical oxygen demand	50,000	Magnesium (Mg)	615.00
Total solid (TS)	40,500	Calcium (Ca)	439.00
Suspended solids (SS)	18,000	Boron (B)	7.60
Total volatile solids	34,000	Iron (Fe)	46.50
Ammoniac nitrogen	35	Manganese (Mn)	2.00
Total nitrogen	750	Copper (Cu)	0.89
		Zinc (Zn)	2.30

CPO contains less than 5% FFA, which is removed during refining, bleaching, and deodorising (RBD) in the refinery as palm fatty acids distillate (PFAD), a by-product of physical refining in the deodorisation stage. *Table 3* shows the PFAD specifications [6]. It indicates that a high percentage (≥95%) of saponifiable matter signifies a high-quality PFAD with a substantial content of usable fatty acids. In PFAD, the majority of fatty acids are palmitic acid (C16:0) and oleic acid (C18:1). These fatty acids are valuable for making soaps, detergents, candles, animal feed, and feedstock for the oleochemical industry. Meanwhile, moisture and impurities in PFAD must be kept at very low percentages to ensure stability, purity, and safety for industrial applications. The FFA content is measured as palmitic acid, the predominant fatty acid in palm oil. At least 70% FFA confirms that PFAD is suitable for normal applications and requires additional treatment processes to produce fatty acid methyl ester (FAME), also known as biodiesel.

Table 3. PORAM Palm Fatty Acids Distillate Specifications

Parameter	Specification Limit
Saponifiable Fatty Matter	95% minimum
Moisture and Impurity (M&I)	1.00% maximum
Free Fatty Acids (as Palmitic)	70% minimum

3. BIOFUEL FROM BIOMASS

Palm biomass can be combusted directly for heat energy due to its calorific value (*Table 4*) [9].

Table 4. Approximate Calorific Value for Palm Biomass

Palm Biomass	Calorific Value	Palm Biomass	Calorific Value
Empty Bunches	18.838 MJ kg^{-1}	Oil palm fronds	15.72 MJ kg^{-1}
Mesocarp Fiber	19.068 MJ kg^{-1}	Oil palm trunks	17.47 MJ kg^{-1}
Kernel Shell	20.108 MJ kg^{-1}		

Mechanical treatment enhances the marketability of biomass fuel. Briquetting technologies improve the physical and combustion properties by converting low-bulk-density biomass into uniform, higher-density solid fuels under high pressure. Pelletising compacts loose biomass into a densified, uniform fuel for energy production.

Thermal treatment improves the energy density of biomass fuel. Torrefaction is a mild thermal treatment of biomass at 200 – 320 °C under atmospheric pressure without oxygen. Hemicellulose degradation forms various non-liquefiable permanent gases and high-oxygen-content condensables. The final solid product, composed mainly of cellulose and lignin, is brittle, hydrophobic, resistant to microbial degradation, and has enhanced energy density. Pyrolysis is the thermal degradation of biomass without oxygen at 350 – 600°C to produce bio-oil, bio-char, and gas using a catalyst. The bio-oil calorific value from empty fruit bunches (EFB) pyrolysis ranged from 24.90 – 31.16 MJ kg^{-1} [10]. Gasification transforms carbon-containing feedstock into a combustible producer gas, also known as syngas, with a small amount of oxygen at 800 – 1200°C [11].

Franz Fischer and Hans Tropsch from Germany developed the Fischer-Tropsch (FT) process in 1925 to convert syngas containing carbon monoxide (CO) and hydrogen (H_2) produced from gasification into liquid hydrocarbons, ideally alkanes (C_nH_{2n+2}), in the presence of a metal catalyst at 150 – 300°C and a pressure of up to several tens of atmospheres, as shown in the following exothermic chemical reaction [12].

$$(2n+1)\ H_2 + n\ CO \rightarrow C_nH_{2n+2} + n\ H_2O;\ \Delta H = -165\ kJ\ (mol)^{-1}\ CO$$

The hydrocarbon chain growth involves a repeated sequence. The water-gas shift reaction adjusted the H_2:CO ratio, providing a hydrogen source at the expense of carbon monoxide.

$$H_2O + CO \rightarrow H_2 + CO_2$$

4. BIOGAS FROM PALM OIL MILL EFFLUENT

Anaerobic POME digestion that produces biogas consists of four (4) metabolic reaction stages involving different types of micro-organisms: hydrolysis, acidification, acetogenesis, and finally, methanogenesis. Many factors influence biogas production, such as temperature, pH, hydraulic retention time (HRT), *etcetera*. Either a continuously stirred tank reactor or a covered lagoon system is preferable for POME with high solids and oil content. On average, 1 m^3 POME produces about 28 m^3 biogas at standard temperature and pressure (STP), 0°C at 100 kPa, with a calorific value of 20 MJ m^{-3}. *Table 5* shows the typical biogas composition [13]. Nevertheless, biogas project proposals are not economically viable for mills with capacities below 45,000 kg h^{-1} due to low carbon loading. *Table 6* presents the estimated power generation potential for various mill

capacities. The raw biogas is treated to remove hydrogen sulfide (H_2S), typically by pressurised water scrubbing, before being used as fuel for internal combustion engines [14].

Table 5. Typical Biogas Composition

Elements	Formula	Concentration [Vol. %]
Methane	CH_4	50–75
Carbon dioxide	CO_2	25–45
Water vapour	H_2O	2–7
Oxygen	O_2	< 2
Nitrogen	N_2	< 2
Hydrogen sulphide	H_2S	< 2
Ammonia	NH_3	< 1
Hydrogen	H_2	< 1

Table 6. Typical Projected Potential Power from POME

Mill Capacity	POME Generated	Potential Power
30,000 kg h^{-1}	21.0 m^3 h^{-1}	1.1 MW_e
45,000 kg h^{-1}	31.5 m^3 h^{-1}	1.6 MW_e
60,000 kg h^{-1}	42.0 m^3 h^{-1}	2.1 MW_e
90,000 kg h^{-1}	63.0 m^3 h^{-1}	3.2 MW_e

5. PALM BIODIESEL FROM FREE FATTY ACIDS

Palmitic acid (C16:0) from PFAD is the perfect feedstock for FAME production in the presence of mild acidic catalysts such as methanesulfonic acid (CH_4O_3S), as shown in the chemical reaction known as esterification, which is practically only feasible with excessive methanol at 65ºC under atmospheric pressure [15].

$$\underset{\text{Palmitic acid}}{C_{16}H_{32}O_2} + \underset{\text{Methanol}}{CH_4O} \xrightarrow{CH_4O_3S} \underset{\text{Methyl Palmitate}}{C_{17}H_{34}O_2} + \underset{\text{Water}}{H_2O}$$

The first-order reaction rate based on the disappearance of a single reactant, *X*, could be expressed as

$$-\frac{d(X)}{dt} = k(X) \tag{1}$$

Solving the rate law equation above yields

$$\int \frac{1}{X} dX = \int -k dt \tag{2}$$

$$\ln(X) = -kt + C; \quad \text{At } t = 0, X = X_0 \text{ thus } C = \ln(X_0) \tag{3}$$

$$\ln(X) = -kt + \ln(X_0) \tag{4}$$

The ln(*X*) versus *t* plot for a first-order reaction is a straight line with slope -*k* crossing the vertical axis at ln(X_0), where *t* is reaction time, and X_0 is the initial amount of reactant. The second-order reaction rate is

$$-\frac{d(X)}{dt} = k(X)^2 \tag{5}$$

Solving the rate law equation above yields

$$-\int \frac{1}{X^2} dX = \int k dt \tag{6}$$

$$\frac{1}{X} = kt + C; \quad \text{At } t = 0, X = X_0 \text{ thus } C = \frac{1}{X_0} \tag{7}$$

$$\frac{1}{X} = kt + \frac{1}{X_0} \tag{8}$$

The $\frac{1}{X}$ versus *t* plot for a second-order reaction is a straight line with slope *k,* crossing the vertical axis at $\frac{1}{X_0}$. Based on the courtesy laboratory data (Nur *et al.*, 2015), the reaction rate analysis (*Figure 1*) indicates the overall reaction tends to second order with respect to FFA.

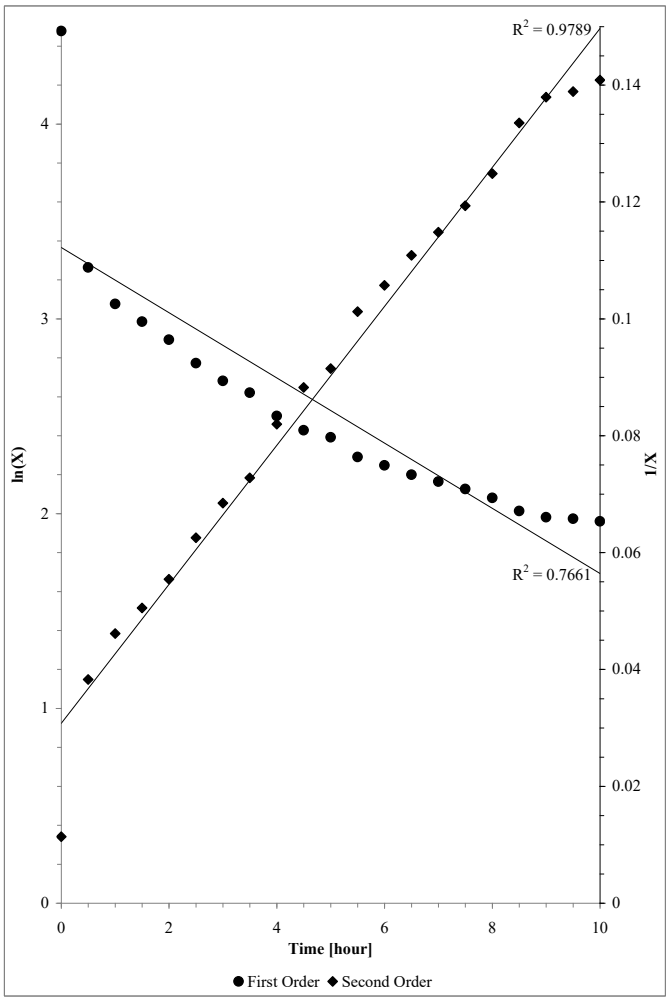


Fig. 1. Overall Reaction Rate Analysis with Respect to Free Fatty Acids

The second-order behaviour reflects the bimolecular nature of the esterification step. An FFA molecule and an alcohol molecule must interact to form the ester. Increasing either reactant concentration can therefore increase the reaction rate. Kinetic analysis of empirical data indicated that the forward reaction is pseudo-first order with respect to FFA when methanol is in excess. In contrast, the reverse reaction is second order with respect to methyl ester and water. The temperature-dependent reaction rate constants, expressed in the Arrhenius equation for the respective reactions, are shown in *Equation (9)*, where r_c denotes the reaction rate, k_a is the forward reaction rate constant, k_b is the reverse reaction rate constant, and *T* is the reaction temperature [16]. Excess methanol forms a methanol-water mixture that can be recovered via distillation.

$$r_c = k_a[\text{FFA}] - k_b[\text{FAME}][\text{Water}]$$
$$k_a = 6.82e^{-\frac{18.772}{RT}} \tag{9}$$
$$k_b = 50.01e^{-\frac{38.126}{RT}}$$

where R is universal gas constant = 8.314463 J $K^{-1}mol^{-1}$ and T in [K].

Due to limitations in the software databank, the FFA esterification reaction simulation used oleic acid (39.2%) instead of palmitic acid (44.0%) as the reactant. *Table 7* presents the physical properties of all compounds involved in the esterification reaction.

Table 7. Physical Properties of Reaction Compound

Compound	Oleic Acid	Methanol	Methyl Oleate	Water
Chemical Formula	$C_{18}H_{34}O_2$	CH_4O	$C_{19}H_{36}O_2$	H_2O
Molecular Weight	282.47	32.04	296.50	18
Specific Gravity	0.895	0.756	0.874	1.000
Boiling Point	360°C	64.7°C	218.5°C	100°C

Note: Molecular Weight unit is [g mol^{-1}]

Based on a 60-tonne mill with a 20% oil extraction rate (OER) and 5% FFA content, a fully efficient separation process produces 600 kg h^{-1} of FFA. Thus, the feed stream in the simulation consists of 2.1241 kmol h^{-1} of oleic acid and 4.2482 kmol h^{-1} of methanol.

Methyl oleate is insoluble in water, oleic acid is miscible with methanol, and methanol is soluble in water. Thus, two immiscible liquid layers form at the end of the esterification. Methyl oleate and unreacted oleic acid form the top layer, while a water-methanol mixture forms the bottom. Excessive methanol is then recovered via distillation.

The methanol-water mixture is assumed to be in equilibrium with the vapour phase in the distillation column. Raoult's Law and Dalton's Law determine the relative volatility.

Fenske formula (*Equation (10)*) determines the minimum distillation stages, N_m, required to achieve a specified separation at total reflux, where α is the relative volatility, x_H is the heavy key fraction in liquid, and x_L is the light key fraction in liquid. Recommended distillation stages are $2.5N_m$. A detailed calculation is provided in the **Appendix**.

$$N_m = \frac{\ln(S_F)}{\ln(\alpha)} \quad \text{where} \quad S_F = \frac{\left(\frac{x_L}{x_H}\right)_D}{\left(\frac{x_L}{x_H}\right)_B} \tag{10}$$

Figure 2 illustrates a preliminary computer-aided process simulation schematic diagram. The raw materials, oleic acid and excess methanol (stream 01), are fed to the esterification reactor (R1) to produce FAME (biodiesel) and water as a by-product. The reaction product (stream 02) is transferred to the separator (S1) to recover FAME (stream 03). The remaining water-methanol mixture (stream 04) is then transferred to the distillation column (D1). The distillation column separates methanol from water. The top product (stream 05) is methanol-rich, and the bottom product (stream 06) is water with residual methanol. *Table 8* summarises the simulation results.

FAME, as palm biodiesel, can be used in pure form (B100) but is usually blended with petroleum diesel at a specified percentage. Malaysia began mandatory palm biodiesel blending with the B5 programme (5% palm biodiesel blended with 95% fossil diesel) in June 2011, covering the transport and fisheries sectors. This was followed by the B7 programme in October 2014 and the B10 programme in February 2019. Langkawi, Labuan, and Sarawak launched the B20 programme in January 2020, but it has not yet been implemented nationwide. For the industry sector, the mandatory use of B7 has been in place since July 2019. The Malaysian Palm Oil Board (MPOB) conducted a pilot project using B20 biodiesel for ground service vehicles at Kuala Lumpur International Airport in February 2025. Life cycle studies on biodiesel also show that greenhouse gas (GHG) emissions are reduced by up to 70% compared to conventional diesel. In fact, the B20 programme reduces atmospheric sulphur emissions by up to 100 tonnes annually because biodiesel is a sulphur-free fuel. In line with mitigation efforts, Malaysia has actively introduced renewable energy sources such as palm biodiesel to reduce carbon emissions, especially in the aviation sector. SD Guthrie launched the B30 biodiesel pilot project for Carey Island plantation operations on 18 July 2025, in collaboration with the Ministry of Plantation Industries and Commodities (KPK), PETRONAS Dagangan Bhd (PDB), and MPOB. The project reduces GHG emissions by up to 23% per litre compared to conventional diesel.

6. SUSTAINABLE AVIATION FUEL

Due to the rapid growth of worldwide air traffic, the International Air Transport Association (IATA) aimed to reduce 50% of the 2005 annual aeronautical CO_2 emissions by 2050. Sustainable aviation fuel (SAF) for commercial aviation could be produced from biomass and waste feedstocks via various pathways, depending on the renewable feedstock [17]. *Figure 3* describes palm-based feedstock pathways for SAF production. Palm-derived feedstock, such as CPO, sludge palm oil (SPO), and palm biomass, offers multiple viable pathways for SAF production with considerable potential for greenhouse gas (GHG) emissions reduction. SAF can be produced via the hydrotreated esters and fatty acids (HEFA) pathway, where CPO and sludge oil are pretreated before further conversion in the HEFA process. This widely recognised SAF pathway involves hydrotreating, isomerisation, and fractionation to produce a drop-in fuel known as HEFA-Synthetic Paraffinic Kerosene (SPK). HEFA-SPK from palm-based sources offers over 80% GHG savings, although it requires quality control and compliance with ASTM standards. Meanwhile, advanced HEFA-SPK derived through emerging or unapproved methods (e.g., from pyrolysis oils) also demonstrates high emission savings (>80%). Additionally, palm biomass pyrolysis produces bio-oil, which is then integrated into the HEFA process after pretreatment. This offers an alternative route for utilising non-edible lignocellulosic residues, potentially improving feedstock sustainability and reducing the impacts of land-use change. Alternatively, palm biomass gasification produces syngas, a mixture of carbon monoxide and hydrogen, which is then purified and converted via the thermochemical Fischer-Tropsch (FT) pathway, followed by hydrocracking to yield FT-SPK. This ASTM D7566 pathway offers the highest GHG savings, above 85%. It supports the use of waste biomass, making it a promising route for future SAF production aligned with circular bioeconomy principles.

The aviation fuel specification is certified to ASTM

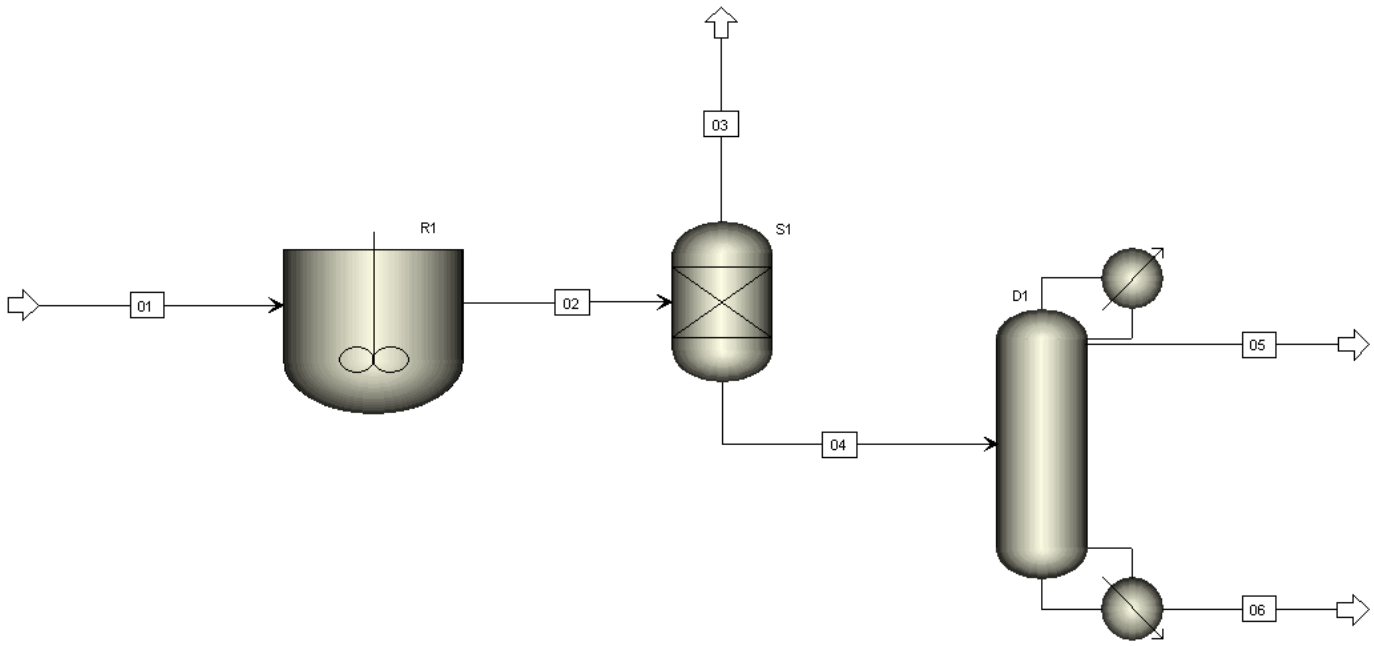


Fig. 2. Computer-Aided Simulation Methyl Ester Preliminary Process Flow Diagram

Table 8. Summary of results generated from process simulation output

Stream	01	02	03	04	05	06
Mole Flow			kmol s^{-1}			
Oleic acid	5.90028E-4	1.16219E-5	1.16219E-5	0.0	0.0	0.0
Methanol	1.18006E-3	6.01650E-4	0.0	6.01650E-4	5.59699E-4	4.19508E-5
Methyl Ester	0.0	5.78406E-4	5.78406E-4	0.0	0.0	0.0
Water	0.0	5.78406E-4	0.0	5.78406E-4	3.03290E-5	5.48077E-4
Total Flow	**1.77008E-3**	**1.77008E-3**	**5.90028E-4**	**1.18006E-3**	**5.90028E-4**	**5.90028E-4**
Mass Flow			kg s^{-1}			
Oleic acid	0.1666632	3.28279E-3	3.28279E-3	0.0	0.0	0.0
Methanol	0.0378115	0.0192781	0.0	0.0192781	0.0179339	1.34419E-3
Methyl Ester	0.0	0.1714937	0.1714937	0.0	0.0	0.0
Water	0.0	0.0104201	0.0	0.0104201	5.46385E-4	9.87376E-3
Total Flow	**0.2044748**	**0.2044748**	**0.1747765**	**0.0296983**	**0.0184803**	**0.0112179**
Temperature	338.1500 K	343.1500 K	343.1500 K	349.2684 K	338.4728 K	363.4619 K
Pressure [Nm^{-2}]	1.01325E+5	1.01325E+5	1.01325E+5	1.01325E+5	1.01325E+5	1.01325E+5
Vapor Frac	0.0	0.0	0.0	0.0	0.0	0.0
Liquid Frac	1.0	1.0	1.0	1.0	1.0	1.0
Solid Frac	0.0	0.0	0.0	0.0	0.0	0.0
Density [kg m^{-3}]	844.3211	823.1886	839.4860	790.3213	751.6080	894.9517
Average *MW*	115.5170	115.5170	296.2174	25.16686	31.32114	19.01259
Enthalpy [J kg^{-1}]	-3.6553E+6	-3.5033E+6	-2.3738E+6	-1.0232E+7	-7.5596E+6	-1.4598E+7
Entropy [$J(kgK)^{-1}$]	-6319.119	-6266.391	-6111.127	-7372.304	-7108.933	-8002.877

D1655 as shown in *Table 9*. The Fischer-Tropsch process produces straight paraffinic jet fuel (SPK) and additional aromatic compounds (SAK) with a maximum blending ratio of 50% with fossil-based kerosene into Jet A1 jet fuel. ASTM has two (2) different certified processes to produce D7566 Annex 1 straight paraffinic jet fuel (SPK) and D7566 Annex 4 additional aromatic compounds (SAK). SPO does not face food-fuel issues if used as a feedstock for sustainable energy generation. Deoxygenates triglycerides and FFA under moderate conditions (300 − 400 °C and H_2 pressure of 20 − 50 bar) using hydrogen and suitable catalysts in the hydrotreated esters and fatty acids (HEFA) process, producing straight paraffin for alternative aviation fuels [18]. Approximately 50,000 tonnes of SPO are generated annually. PETRONAS is cooperating with Malaysian palm oil producers, including Felda Global Venture (FGV) and SD Guthrie, to develop palm oil waste-based SAF.

Table 9. Aviation Fuel Specification

	Jet A-1	Jet A
Flash point	38°C (100°F)	38°C (100°F)
Autoignition temperature	210°C (410°F)	210°C (410°F)
Freezing point	−47°C (−53°F)	−40°C (−40°F)
Max adiabatic burn temperature	2,230°C; open-air burn temperature: 1,030°C	
Density at 15°C (59°F)	0.804 kg L^{-1}	0.820 kg L^{-1}
Specific energy	43.15 MJ kg^{-1}	43.02 MJ kg^{-1}
Energy density	34.7 MJ L^{-1}	35.3 MJ L^{-1}

The HEFA described in *Figure 4* produces alkanes with the main compositions of C_{16}, C_{17}, C_{18}, and C_{19} (*Table 10*) from palm oil fatty acids [19]. Hydrocracking and hydro-isomerising were required to split the straight paraffinic molecules into C_8

to C_{16} kerosene-length molecules for blending up to 50% as SAF based on ASTM D7566 Annex 2.

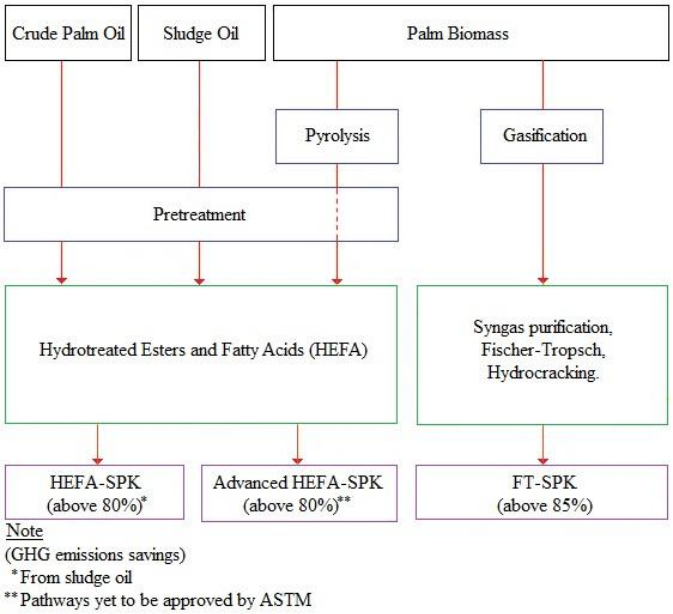


Fig. 3. Sustainable Aviation Fuel Production Pathways

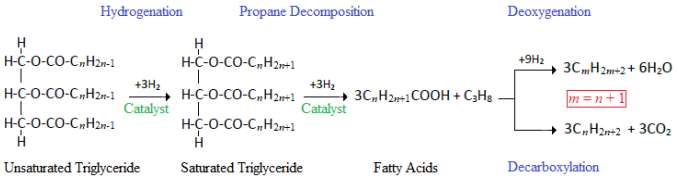


Fig. 4. Hydrotreated Esters and Fatty Acids (HEFA) to produce Straight Paraffin

Table 10. Palm Oil Fatty Acids and Triglyceride Compositions

Compositions	%wt.	Triglyceride carbon number	%wt.
Lauric acid (C12:0)	0.2	C46	1.2
Myristic acid (C14:0)	1.1	C48	8.1
Palmitic acid (C16:0)	44.1	C50	39.9
Palmitoleic (C16:1)	0.2	C52	38.8
Stearic acid (C18:0)	4.4	C54	11.4
Oleic acid (C18:1)	39.0	C56	0.6
Linoleic acid (C18:2)	10.6		
Linolenic acid (C18:3)	0.3		
Arachidic acid (C20:0)	0.2		

Cracking is an endothermic process that breaks down long-chain hydrocarbons into simpler molecules at high temperatures. Hydrocracking is a catalytic process that uses hydrogen to break high-energy C-C bonds (377 kJ mol^{-1}), facilitated by a bifunctional catalyst. Since aviation fuel operating temperatures are generally lower than those of ground-based transport, hydro-isomerisation improves the cold properties of renewable hydrocarbons in *n*-alkanes, such as pour point and cold filter plugging point (CFPP), with significantly less fuel loss than conventional methods [20].

7. SOLAR ENERGY

Solar irradiance is the electromagnetic radiation power per unit area [kW m^{-2}] received from the Sun. A peak sun hour is defined as a one-hour period during which solar irradiance produces 1 kWh of energy per square meter of surface area [kJ m^{-2}]. Geographical and physical locations influence the available amount of sunlight. Malaysia is an equatorial country with abundant sunshine year-round, with mean daily solar radiation ranging from 4.7 to 6.5 kWh m^{-2} or 400 to 600 MJ m^{-2} per month [21]. Solar energy is a promising clean energy source that does not generate any pollutants or greenhouse gases (GHG). In 2020, Malaysia had 457 palm oil mills, 42 palm kernel crushers, 50 refineries, 20 oleochemical plants, and 19 biodiesel plants [22]. The rooftops of palm oil industrial premises offer significant space for solar panels.

Semiconductors are typically made of silicon. The characteristic of electric current generation when exposed to light is known as the photovoltaic effect. Solar photovoltaic (PV) technology is a renewable energy technology in which solar cells convert sunlight directly into electricity through the photovoltaic effect (*Figure 5*).

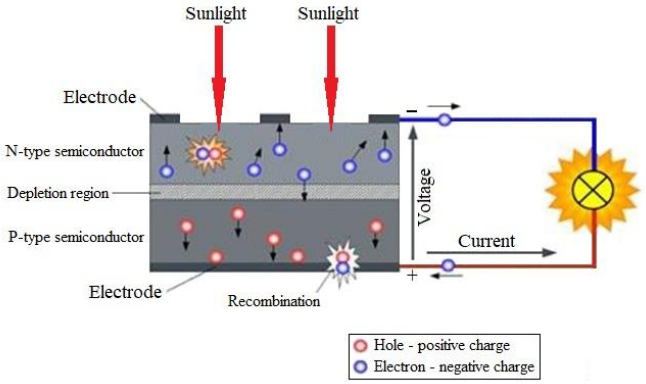


Fig. 5. Solar cell working principle

A solar cell is made of a layer of *p*-type semiconductor placed next to a layer of *n*-type semiconductor. The *p*-type semiconductor is produced by adding atoms such as boron or gallium into a silicon matrix, resulting in an excess of positively charged holes. The *n*-type semiconductor is created by incorporating atoms such as phosphorus into a silicon matrix, resulting in an excess of negatively charged electrons. Two layers form a depletion zone near the junction where electrons in the *n*-type layer move into holes of the *p*-type layer. When all holes are filled with electrons in the depletion zone, the *p*-type side of the depletion zone will contain negatively charged ions, while the *n*-type side of the depletion zone will contain positively charged ions, hence creating an internal electric field barrier that prevents the *n*-type layer electrons from filling holes in the *p*-type layer.

When sunlight strikes a solar cell, photons excite electrons in the semiconductor. The escaping electrons leave holes behind. The electric field drives electrons to the *n*-type layer and holes to the *p*-type layer. If a wire connects the *n*-type and *p*-type layers, electrons flow from the *n*-type layer to the *p*-type layer by crossing the depletion zone and then flow through the external wire back to the *n*-type layer, creating an electric current. A common single-junction silicon solar cell can produce a maximum open-circuit voltage of approximately 0.5 to 0.6 volts and generate a current of 28 to 40 mA cm^{-2}. Thus,

multiple solar cells are connected to form a solar module, and multiple modules are connected to form a solar panel (*Figure 6*) to generate the required electricity in a typical design.

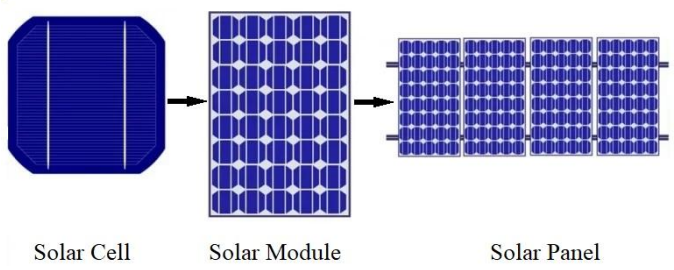


Fig. 6. Solar panel building blocks

An inverter converts the direct current (DC) generated by solar panels into alternating current (AC) before distribution. Solar power generation depends on variable sunlight, and cloudy or rainy weather reduces output. Thus, batteries are often used for energy storage to ensure a continuous power supply. *Figure 7* illustrates a scalable basic solar photovoltaic system that meets energy needs.

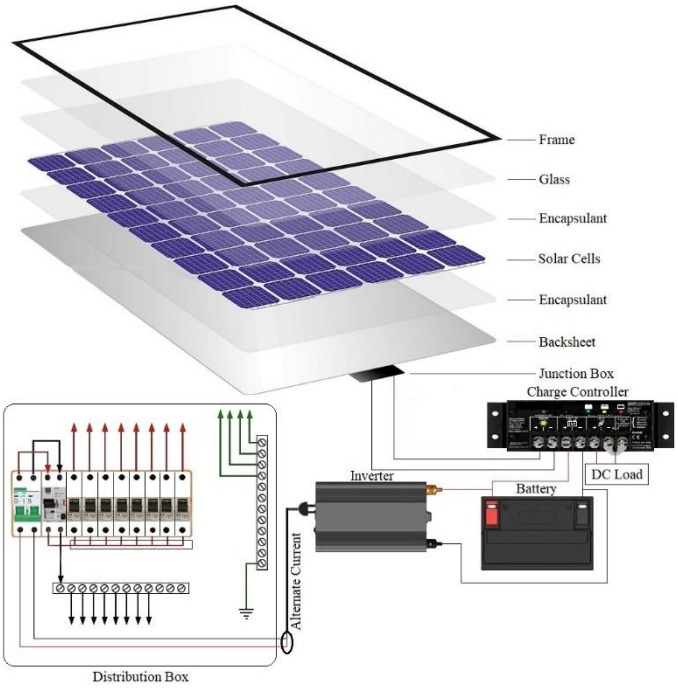


Fig. 7. Basic photovoltaic solar system schematic diagram

8. DISCUSSION

Malaysia has approximately 5.89 million hectares of oil palm plantations, producing around 94.7 million tonnes of lignocellulosic biomass with various potential uses, including biochemical products, fertilisers, and biofuels. This makes Malaysia one of the most promising destinations for biomass-based investments. According to the Malaysian Investment Development Authority (MIDA), the total approved investments in 2023 reached RM31.7 million. *Figure 8* illustrates the Malaysian oil palm plantation area and crude palm oil production from 1975 to 2022. The FFB yield in 2022 was 15.49 tonnes per hectare. Factors such as planting areas, weather conditions, pests, and disease outbreaks can affect crude palm oil yield. The quality and quantity of palm oil cannot be improved beyond the natural oil content of the fruits, although mills work to reduce processing losses. Therefore, the feedstock availability for renewable palm biofuel depends on the plantation area, which is constrained by land availability. Malaysian solid biofuels and renewable waste capacity was approximately 0.78 gigawatts in 2023, based on published data from Statista.

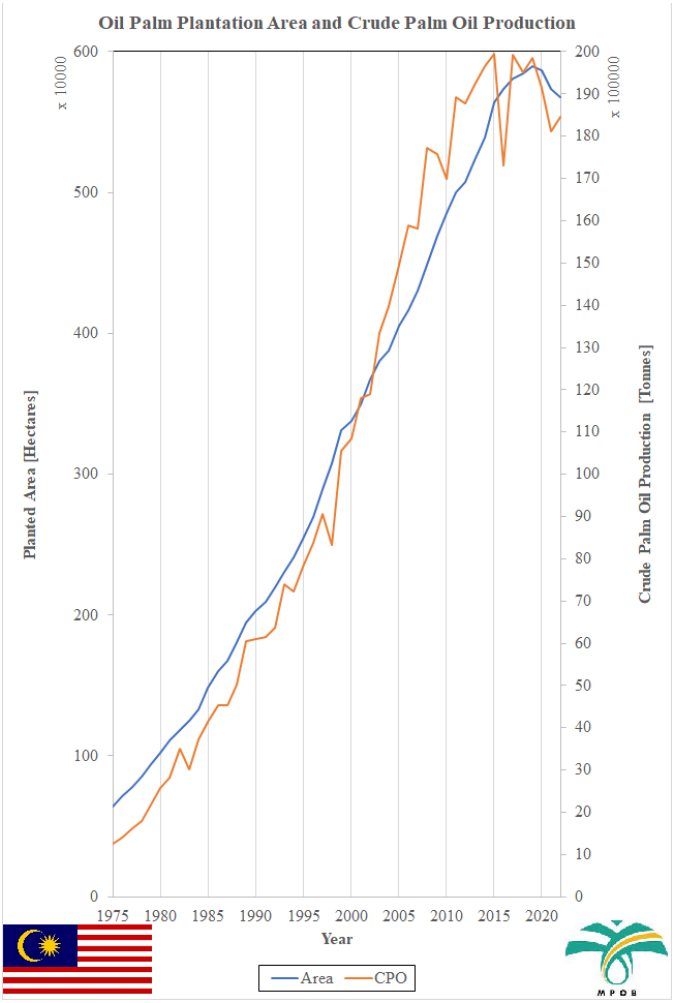


Fig. 8. Malaysian Oil Palm Plantation Area and Crude Palm Oil Production

Malaysian oil palm cultivation land base is approaching a practical ceiling. Future growth must therefore come primarily from higher yields, improved residue recovery and greater conversion efficiency rather than from opening new plantations. Hence, palm bioenergy remains unscalable beyond the existing plantation system.

The food–fuel conflict arises when crops or agricultural products that could otherwise be used for human consumption are diverted into fuel production. POME, SPO, and PFAD instead make fuel production a form of waste or by-product.

The Malaysian government is allocating RM10 million as seed funding to guarantee demand for locally produced carbon credits, aiming to stimulate the market and support the journey towards achieving national net-zero emissions by 2050. Meanwhile, approximately 20 per cent of renewable energy capacity is expected to be completed by 2025. Sustainability issues are inevitable in renewable energy initiatives involving various policies. The Malaysian Sustainable Palm Oil (MSPO)

chain of custody (CoC) for oil palm biomass (MS 2751:2022) was launched in March 2022 to ensure the sustainability of palm biomass for renewable energy. However, an international sustainable certification, the Green Gold Label (GGL), established in 2002 by the Green Gold Label Foundation for biomass and bioliquids used in biobased chemicals, electricity, and heat production, is crucial for export markets, particularly in Japan and Europe. GGL essentially bridges a physical biomass product and a credible sustainability claim. For Japan, GGL is recognised within the Feed-in Tariff (FIT) / Feed-in Premium (FIP) regulatory framework, including agricultural residues and relevant palm-derived materials. For Europe, GGL is potentially important as a sustainability and traceability framework, but EU RED recognition should be treated separately until the European Commission formally recognises the relevant GGL module.

Palm oil mills consume about 0.061 kWh of energy to process 1 kg of FFB, with the energy derived from a biomass mixture of mesocarp fibre and kernel shell. Besides renewable energy utilisation, environmental issues such as particulate emissions must be addressed to meet sustainability requirements. Under global green energy policies, the quoted price of palm kernel shell was recently recorded at USD 0.15 per kg.

The European Union Renewable Energy Directive guarantees that crops used for biofuel production are sustainable and do not cause deforestation through indirect land-use change (ILUC), without specifying particular biofuels or feedstocks. The ILUC assessment factor is based on the energy content of traded products from different annual crops compared to palm oil. Unfortunately, oil palm has been linked to the highest level of deforestation according to data from 2008 to 2015. Nonetheless, certified low ILUC-risk palm oil still benefits from incentives. Exemptions include planting on unused land, and smallholders with a threshold of two (2) hectares are granted privileges.

FAME contains 11% oxygen, tends to solidify at low temperatures and is generally unsuitable as aviation turbine fuel. Hydrotreated esters and fatty acids (HEFA) convert the same types of lipid feedstocks into oxygen-free hydrocarbon molecules that can meet aviation-fuel requirements. Both biofuels have different characteristics, especially cloud point [23], which is insignificant for ground-based transportation but may cause a disaster in aviation applications, especially at high altitudes. As a result, FAME and HEFA could be used as ground-based transportation fuel, but only HEFA can be used as sustainable aviation fuel (SAF).

Life cycle assessment (LCA) technique evaluates environmental impacts at every stage of a product or service, from raw material processing and manufacturing through distribution, use, repair, maintenance, and disposal or recycling. ISO 14040 and 14044 outline the general procedures, requirements, and terminology. The Global Warming Potential (GWP) for biogenic methane, also known as biogas, is 27.75 kg $CO_{2\text{-eq}}.kg^{-1}$ [24] as a characterisation factor used to translate biogenic methane emissions into CO_2-equivalent emissions in LCA methodologies for POME assessment. Methane leakage can dominate the climate impact of wastewater treatment, while capturing and utilising that methane can substantially improve the calculated life-cycle GHG performance. Since January 2014, biogas capture has become an additional licensing requirement for new and expanding mill capacities in Malaysia to help reduce LCA carbon footprints. Nonetheless, all existing mills are encouraged to adopt biogas capture voluntarily. Biogas is gaining momentum in Malaysia, with an estimated potential of approximately 500 MW [25], even though the plant installation progress is slower than solar photovoltaic (PV) [26].

Besides being inexpensive and widely available, the materials used in solar cells must possess high optical absorption, high electrical conductivity, and a band gap close to 1.5 electron volts, such as silicon (Si), gallium arsenide (GaAs), cadmium telluride (CdTe), and copper indium selenide ($CuInSe_2$). The initial CAPEX investment remains substantial currently, although prices for solar photovoltaic systems have declined over the years. However, solar photovoltaic technology continues to grow in popularity and improve through technological advancements because of low OPEX and no pollutants, making it an increasingly important part of the global energy mix and the transition to cleaner energy sources.

A palm oil industrial site may have extensive roof area across its mill buildings, warehouses, workshops and processing facilities. However, management may be reluctant to commit substantial capital to an asset that is outside the core business. The investment also competes with other priorities such as mill upgrades, production expansion, facilities for oil loss reduction, effluent treatment, and methane capture. The initial CAPEX barrier should therefore be treated as a financing-structure problem. For a palm-oil industrial premises, the most compelling approach may be a third-party Power Purchase Agreement (PPA) or solar leasing model, allowing the mill to utilise its substantial rooftop area without committing huge capital. Malaysia's current Solar ATAP programme explicitly supports both structures and describes them as zero-upfront-CAPEX options. The strongest investment proposal would therefore present three cases side-by-side (outright ownership, bank-financed ownership, and zero-CAPEX PPA/lease) and separately compare net present value (NPV), investment return rate (IRR), cumulative savings and GHG reduction for 15 to 25 years. The main obstacles to installing rooftop solar PV are not whether the system is technically viable, but the large upfront capital expenditure (CAPEX) required before any electricity savings are realised.

The Malaysian Government provided the Green Investment Tax Allowance (GITA) and Green Income Tax Exemption (GITE) incentives until 2023. However, the 2024 National Budget announced a revision to the Green Technology Tax Incentive. The Green Technology Financing Scheme 2.0 (GTFS 2.0) is a financing scheme offered to government-supported investors with a 2% per annum interest rate subsidy for the first seven years, along with a 60% government guarantee of the green component cost to financial institutions.

9. CONCLUSION

As the national energy transition moves towards cleaner and more sustainable energy sources, the Malaysian oil palm industry should consider several initiatives for the future.

Palm oil milling and downstream processing should utilise renewable energy in daily routine operations to reduce dependence on fossil fuels, even though some initial capital investment, such as solar system installation, will be inevitable. Circular economy practices that minimise waste and maximise resource efficiency by reducing, recycling, and reusing

industrial by-products, such as POME, to generate biogas for energy production need to be implemented efficiently. Advocate for and comply with government regulations and policies that may benefit the industry, such as the Green Investment Tax Allowance (GITA), which provides a tax allowance incentive equivalent to 100% of qualifying capital expenditure (QCE) incurred on green assets. Continuous international collaboration in research and development to enhance industrial sustainability, such as exploring new technologies for alternative by-product usage, is crucial for addressing global challenges.

The success of the national energy transition in the oil palm sector requires a comprehensive, collaborative approach from all stakeholders, including government, businesses, local communities, and consumers.

REFERENCES

[1] IRENA, Asia and Pacific Overview. United Arab Emirates: *International Renewable Energy Agency*, 2023. url: https://www.irena.org/How-we-work/Asia-and-Pacific#overview

[2] EPA, Sources of Greenhouse Gas Emissions Overview, 2023. United States: *Environmental Protection Agency*. url: https://climatechange.chicago.gov/ghgemissions/sources-greenhouse-gas-emissions

[3] Wail Gourich, Cher Pin Song, Kiat Seng Qua, and Eng-Seng Chan. (2023). The potential of palm bioenergy in achieving Malaysia's renewable energy target and climate ambition in line with the Paris Agreement. *Energy for Sustainable Development* 76: 101296. doi: https://doi.org/10.1016/j.esd.2023.101296

[4] Siti Mashani Ahmad, Azman Ismail, Noorshamsiana Abdul Wahab, Kamalrudin Mohamed Salleh, Nur Nadia Kamil and Norhidayu Abdullah. (2024) Comparative analysis of current biomass utilisation by palm oil mills in Peninsular Malaysia. *Journal of Sustainability Science and Management*, 19(7): 166 – 176. doi: https://doi.org/10.46754/jssm.2024.07.009

[5] Ng, S. B. (2011). *Understanding Extraction of Palm Oil*. Malaysia: Malaysian Palm Oil Council.

[6] PORAM (2000). *PORAM Standard Specifications for Processed Palm Oil*. Selangor: The Palm Oil Refiners Association of Malaysia. url: https://poram.org.my/wp-content/uploads/2013/12/1.-PORAM-Standard-Specification.pdf

[7] Noorshamsiana, A W; Astimar, A A; Nor Hayati, M; Nor Faizah, J; Mohamadiah, B and Norhayati, S (2013). Optimisation of Enzymatic Sludge Palm Oil Recovery from Palm Oil Mill Effluent using Response Surface Methodology. *Journal of Oil Palm Research* 25(3): 348 – 356.

[8] Fatah Yah A M; Andrew Y K C and Ravindranathan M (2012). Spray Drying Palm Oil Mill Effluent. *Palm Oil Engineering Bulletin*. 100: 11 – 32.

[9] Nasrin, A B; Choo, Y M; Lim, W S; Joseph, L; Michael, S; Rohaya, M H; Astimar, A A; and Loh, S K (2011). Briquetting of Empty Fruit Bunch Fibre and Palm Shell as a Renewable Energy Fuel. *Journal of Engineering and Applied Sciences* 6(6): 446 – 451.

[10] Chin Kit Ling, H`ng Paik San, Eng Hooi Kyin, Lee Seng Hua, Lum Wei Chen, and Chin Yin Yee (2015). Yield and Calorific Value of Bio-Oil Pyrolysed from Oil Palm Biomass and its Relation with Solid Residence Time and Process Temperature. *Asian Journal of Scientific Research*, 8: 351-358. doi: https://doi.org/10.3923/ajsr.2015.351.358

[11] Shah HH, Amin M, Iqbal A, Nadeem I, Kalin M, Soomar AM, Galal AM. (2023). A review on gasification and pyrolysis of waste plastics. *Front Chem*. 10:960894. PMID: 36819712; PMCID: PMC9936530. doi: https://doi.org/10.3389/fchem.2022.960894

[12] Olusola O. James, Biswajit Chowdhury, Adediran Mesubi M., and Sudip Maity (2012). Reflections on the chemistry of the Fischer–Tropsch synthesis. *The Royal Society of Chemistry*. doi: https://doi.org/10.1039/c2ra20519j

[13] Loh, S K; Nasrin A B; Bukhari, N A; Sukiran, M A; Muzzammil, N; Daryl Jay, T; Stasha Eleanor, R A; Mohd Faris, M R; Lim, W S and Choo, Y M (2014). Biogas capture and utilisation from palm oil mill effluent. *MPOB Ministry of Plantation Industries and Commodities*.

[14] Andrew Yap Kian Chung and Ummi Kalsum Hasanah M.N. (2021). Computer-Aided Simulation POME Biogas Purification System. *Jurnal Kejuruteraan* 33(2) 2021: 293-316. doi: https://doi.org/10.17576/jkukm-2021-33(2)-15

[15] Nur Sulihatimarsyila Abd. Wafti, Harrison Lik Nang Lau and Choo Y. M. (2015). Production Technology of Biodiesel from Palm Fatty Acid Distillate Using Mild Acid Catalyst. *Journal of Oil Palm Research*, Volume 27(4): 352 – 359.

[16] Apichat Saejio and Kulchanat Prasertsit. (2018). Kinetics and control of palm fatty acid distillate esterification for feasible biodiesel production. *Songklanakarin Journal of Science and Technology*. 40(1): 79 – 86.

[17] Zanata, M., Tri Wulan Amelia, S., Mumtazy, M.R., Kurniawansyah, F., Roesyadi, A. (2019). Synthesis of Bio Jet Fuel from Crude Palm Oil by HEFA (Hydroprocessed Esters and Fatty Acids) Using Ni-Mo Catalyst Supported by Rice Husk Ash-Based SiO_2; *Materials Science Forum* (964) 193-198. doi: https://doi.org/10.4028/www.scientific.net/msf.964.193

[18] Sisira Fangkoch, Sutida Boonkum, Sakhon Ratchahat, Wanida Koo-amornpattana, Apiluck Eiad-Ua, Worapon Kiatkittipong, Wantana Klysubun, Atthapon Srifa, Kajornsak Faungnawakij, and Suttichai Assabumrungrat (2020). Solvent-Free Hydrodeoxygenation of Triglycerides to Diesel-like Hydrocarbons over Pt-Decorated MoO_2 Catalysts. *ACS Omega* 5, 6956−6966. doi: https://doi.org/10.1021/acsomega.0c00326

[19] Siew Wai Lin and Johari Minal (2007). Palm Oil and Fractions. *OFI Middle East*. url: https://www.soci.org

[20] Schmutzler, F., Zschiesche, C., Titus, J., Poppitz, D., Freiding, J., Rakoczy, R., Reitzmann, A. and Gläser, R. (2021), Hydroisomerization of Renewable and Fossil n-Alkanes over Bifunctional Dealuminated ZSM-5 Catalysts. *Chemie Ingenieur Technik*, 93: 981-989. doi: https://doi.org/10.1002/cite.202000163

[21] Petinrin J. O., and Shaaban M. (2015). Renewable energy for continuous energy sustainability in Malaysia. *Renewable and Sustainable Energy Reviews* 50: 967 – 981. doi: https://doi.org/10.1016/j.rser.2015.04.146

[22] MPOB (2021). *Malaysia Oil Palm Statistics 2020*. 40th Edition. Bangi: Malaysian Palm Oil Board.

[23] CBSCI (2019). HEFA Production and Feedstock Selection. *Canada's Biojet Supply Chain Initiative*.

[24] De Rosa, M. and Schmidt, J. (2022). Life Cycle Assessment of Palm Oil at United Plantations Berhad 2022, Results for 2004-2021. Summary report. *United Plantations Berhad*, Teluk Intan, Malaysia.

[25] Loh, S K; Nasrin, A B; Sukiran, M A; Bukhari, N A; Muzzammil, N; Stasha Eleanor, R A and Astimar, A A (2020). The Future of Biogas in the Malaysian Palm Oil Industry: Why Need Methane Capture? *Palm Oil Developments* No.72: 1 – 7.

[26] Nor Adilla Rashidi, Yee Ho Chai, and Suzana Yusup (2022). Biomass Energy in Malaysia: Current Scenario, Policies, and Implementation Challenges. *Bioenergy Research* 15:1371–1386. doi: https://doi.org/10.1007/s12155-022-10392-7

NOMENCLATURE

Symbol	Particular	SI Unit
k	Reaction rate constant	
k_a	Forward reaction rate constant	
k_b	Reverse reaction rate constant	
r_c	Reaction rate	mol s^{-1}
t	Reaction time	s
x_H	Heavy key fraction	-
x_L	Light key fraction	-
N_m	Minimum distillation stages	-
R	Universal gas constant	J $K^{-1}mol^{-1}$
T	Temperature	°C
X_0	Initial reactant amount	mol
α	Relative volatility	-

APPENDIX. METHANOL-WATER RELATIVE VOLATILITY

According to Raoult's Law, each component's partial pressure of an ideal mixture liquid is equal to the pure component's vapour pressure multiplied by its mole fraction in the mixture, as shown in equation (A1), where p is the system pressure, y_i is the component i mole fraction in an ideal gas mixture, and p_i is the component i partial pressure, p_i^* is the component i vapour pressure, and x_i is the component i mole fraction in the liquid mixture.

$$py_i = p_i = p_i^* x_i \tag{A1}$$

The total solution vapour pressure in equilibrium can be determined by combining Raoult's Law and Dalton's Law of partial pressure, as shown in equation (A2).

$$py_1 + py_2 + \cdots + py_n = p_1^* x_1 + p_2^* x_2 + \cdots + p_n^* x_n \tag{A2}$$

Table A1 shows the saturated pressure for each component in a methanol-water mixture at various temperatures. For the binary system methanol-water mixture at atmospheric pressure,

$$\begin{gathered} p_m^* x_m + p_w^* x_w = p_m^* x_m + p_w^*(1 - x_m) \\ = 101.325 \text{ kPa} \end{gathered} \tag{A3}$$

If the distillation is carried out at 72 ºC atmospheric pressure, determine the methanol and water saturated vapour pressures via linear interpolation of the given data.

Methanol

$$\begin{gathered} \frac{p_m^* - 129.41}{139.55 - 129.41} = \frac{72 - 71.2}{73.1 - 71.2} \\ \frac{p_m^* - 129.41}{10.14} = \frac{0.8}{1.9} \\ p_m^* - 129.41 = 10.14(0.4211) \\ p_m^* = 133.6795 \text{ kPa} \end{gathered} \tag{A4}$$

Water

$$\begin{gathered} \frac{p_w^* - 32.964}{35.772 - 32.964} = \frac{72 - 71.2}{73.1 - 71.2} \\ \frac{p_w^* - 32.964}{2.808} = \frac{0.8}{1.9} \\ p_w^* - 32.964 = 2.808(0.4211) \\ p_w^* = 34.1463 \text{ kPa} \end{gathered} \tag{A5}$$

$$\begin{gathered} 133.6795 x_m + 34.1463(1 - x_m) = 101.325 \\ 99.5332 x_m = 67.1787 \\ x_m = 0.6749 \\ x_w = 1 - x_m = 0.3251 \end{gathered} \tag{A6}$$

Thus,

$$\begin{gathered} py_m = p_m^* x_m; \\ y_m = \frac{p_m^* x_m}{p} = \frac{133.6795 \times 0.6749}{101.325} = 0.8904 \end{gathered} \tag{A7}$$

$$y_w = (1 - y_m) = 0.1096 \tag{A8}$$

The methanol-water mixture's relative volatility, α, is defined as

$$\alpha = \frac{p_m^*}{p_w^*} = \frac{133.6795}{34.1463} = 3.9149 \tag{A9}$$

To achieve a distillate containing $x_L = 0.95$ and $x_H = 0.05$,

$$N_m = \frac{\ln(S_F)}{\ln(\alpha)} \quad \text{where} \quad S_F = \frac{\left(\frac{x_L}{x_H}\right)_D}{\left(\frac{x_L}{x_H}\right)_B} \tag{A10}$$

$$S_F = \frac{0.95/0.05}{0.6749/0.3251} = \frac{19}{2.0760} = 9.1522 \tag{A11}$$

$$N_m = \frac{\ln(9.1522)}{\ln(3.9149)} = \frac{2.2140}{1.3648} = 1.6222 \tag{A12}$$

Table A1. Saturated Pressure for Methanol and Water at Various Temperatures

Temperature [ºC]	Water p_w [kPa]	Methanol p_m [kPa]
64.5	24.521	100.74
65	25.03	102.66
66	26.57	106.73
67.6	28.233	113.68
69.3	30.328	121.06
71.2	32.964	129.41
73.1	35.772	139.55
75.3	39.109	151.28
78	43.866	167.02
81.7	50.94	190.44
84.4	56.577	209.96
87.7	64.477	234.53
89.3	68.417	248.34
91.2	73.598	264.85
93.5	80.227	285.04
96.4	89.254	313.83
100	101.325	351.38

The recommended distillation stages, N, are $2.5N_m$

$$N = 2.5 \times 1.6222 = 4.0555 \text{ Say 5 stages.} \tag{A13}$$